

Discrete intragap Pb states in $\text{Pb}_{1-x}\text{Sr}_x\text{S}$

M. A. Tamor, L. C. Davis, and H. Holloway

Research Staff, Ford Motor Company, P.O. Box 2053, Dearborn, Michigan 48121-2053

(Received 9 May 1983)

We observe intragap Pb states in the alloy semiconductor $\text{Pb}_{1-x}\text{Sr}_x\text{S}$. Absorption spectroscopy shows that $\text{Pb}_{1-x}\text{Sr}_x\text{S}$ has an energy gap which decreases from 4.6 eV at $x=1$ to 0.4 eV at $x=0$. At very small Pb concentration ($x=0.993$) a discrete absorption peak appears at 3.5 eV. As the Pb content is increased, this absorption grows in strength and a second peak appears at 3.2 eV. These peaks are ascribed to isolated Pb atoms and Pb dimers, respectively. When the samples are cooled to 80 K the linewidths decrease by 40%. This improved definition reveals a third, very small absorption peak at 3.1 eV, possibly due to a Pb trimer. These results may be interpreted in terms of a simple tight-binding model that predicts an *s*-like impurity state above the valence band. This state is localized on the S atoms surrounding the Pb atom. Also, a *p*-like state due to the Pb 6*p* orbitals exists below the conduction band. Transitions from the *s* to the *p* state account for the impurity spectra.

It was recently demonstrated that the alloy semiconductor $\text{Pb}_{1-x}\text{Sr}_x\text{S}$ may be produced over the entire composition range from SrS to PbS.¹ In that work the room-temperature band gap E_g was found to vary from 4.6 eV at $x=1$ (SrS) to 0.4 eV at $x=0$ (PbS). In addition, discrete absorption lines were observed at 3.5 and 3.2 eV in a sample with $x=0.95$. In the present work the nature of these discrete optical-absorption lines is examined in a series of samples with composition ranging from $x=1.0$ to 0.93.

The details of the sample preparation and characterization methods appear in Ref. 1. It will suffice here to note that the samples were thin films produced by vacuum deposition onto cleaved BaF_2 substrates. Absorption spectra were recorded using a Carey Model 14 spectrophotometer. A liquid-nitrogen cryostat equipped with a cold finger and BaF_2 windows was used to record spectra with the sample cooled to 80 K.

EXPERIMENTAL RESULTS

Figures 1(a) and 1(b) show room-temperature absorption spectra of samples with $x=0.985$ and 0.95. The figures show the square of the absorbance ($(\alpha d)^2$, where α is the inverse absorption length and d is the sample thickness) as a function of photon energy. The absorbance was obtained from the measured optical attenuation [$\log_{10}(I_0/I)$, where I_0 and I are the incident and transmitted light intensities] by correcting for the total reflectivity of the sample-substrate combination. This correction was performed by subtracting the absorbance measured at a photon energy much smaller than the band-gap energy. There is variation of this low-energy baseline due to interference within the thin film. The midpoint of the interference oscillations was taken as the offset value. The magnitude of the oscillations was small compared to the total correction so the approximation is adequate. The use of the constant baseline assumes that the real part of the index of refraction does not vary significantly as the photon energy passes through the band edge. This is the major source of

error in determining the true absorption spectrum. Elimination of this error would require more elaborate spectroscopy than was performed here.

The high-energy portion of each spectrum of $(\alpha d)^2$ vs $h\nu$ defines a straight line. This corresponds to an $(h\nu - E_g)^{1/2}$ dependence in α . This is characteristic of a direct energy gap. The extrapolation of the line to the energy axis marks the value of E_g . It is important to note that theoretical calculations² indicate that the band gap of SrS is indirect and lies at an energy considerably lower than 4.6 eV. Optical absorption due to this indirect transition was not observable in our data. The energy gap of $\text{Pb}_{1-x}\text{Sr}_x\text{S}$ decreases very rapidly with increasing Pb content.

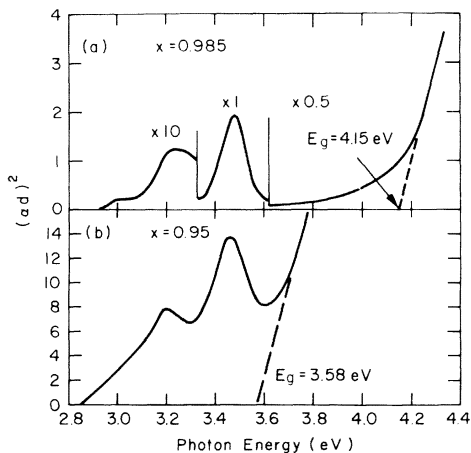


FIG. 1. Room-temperature absorption spectra for 2 μm thick $\text{Pb}_{1-x}\text{Sr}_x\text{S}$ films. (a) $x=0.985$. With only 1.5 at.% Pb, E_g is reduced by almost 0.5 eV from that of SrS (4.6 eV). The curve is rescaled in three regions to emphasize the features of interest. The shoulder at 3.0 eV is due to interference effects within the film and is not an absorption feature. (b) $x=0.95$. E_g is further reduced but the absorption peaks have shifted only slightly. The two peaks are now comparable in magnitude.

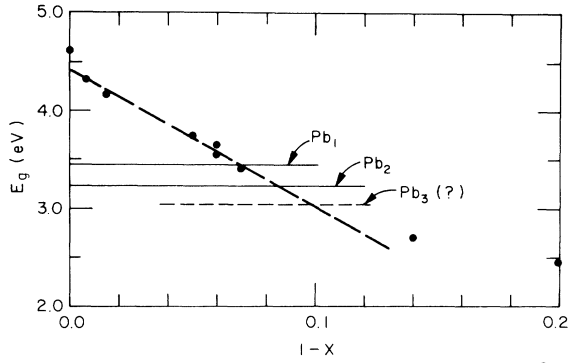


FIG. 2. Composition dependence of E_g in $\text{Pb}_{1-x}\text{Sr}_x\text{S}$. The lines labeled Pb_1 and Pb_2 mark the energies of the discrete absorption peaks. The dashed line labeled Pb_3 marks the position of the third absorption peak visible only at low temperature in samples with $x \leq 0.95$.

Figure 2 shows the value of E_g for $1.0 > x > 0.8$. Visible in Figs. 1(a) and 1(b) are the discrete absorption peaks noted in Ref. 1. The lines grow stronger as the Pb content is increased. The absorbance of the 3.2-eV peak (α_2) increases much more rapidly than that of the 3.5-eV peak (α_1). Only the 3.5-eV line is visible in a sample with $x=0.993$. We ascribe the 3.5-eV absorption line to a localized excitation of isolated Pb atoms in the SrS lattice.

The absorption at 3.2 eV is ascribed to excitation of a state localized to an adjacent pair of Pb atoms. In the NaCl-type SrS lattice, the adjacent Pb atoms will lie along a $\langle 110 \rangle$ or $\langle 100 \rangle$ crystal axis. Assuming that the film grows as a random alloy, the probability of Pb dimer formation should vary as the square of the Pb concentration. Furthermore, the ratio of the dimer to the monomer absorption strength should be linear with the Pb concentration: $\beta\alpha_2/\alpha_1 = 1-x$, where β is an empirical parameter. This measure is useful in comparing different samples because it is not dependent upon sample thickness. To test the dimer hypothesis, we use a crude background subtraction to determine the value of β (Fig. 3). The encroachment of the shifting band edge makes the choice of background difficult. However, the variation of β with com-

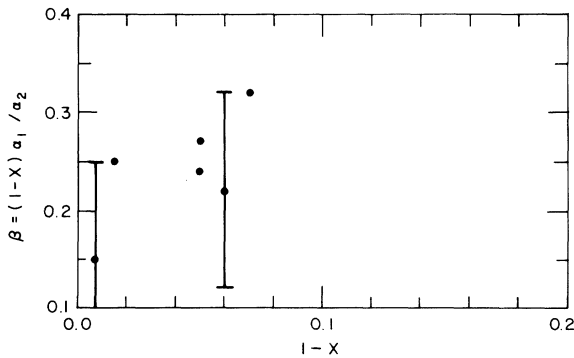


FIG. 3. Composition dependence of the empirical parameter $\beta = (1-x)\alpha_1/\alpha_2$, where α_1 and α_2 are the absorbances of the 3.5- and 3.2-eV absorption lines. Within the estimated errors, β does not vary with composition. This supports the hypothesis that the 3.2-eV absorption peak is due to Pb dimers.

position was found to be quite insensitive to the background correction. Figure 3 shows that within experimental error β remains constant as the Pb content increases tenfold from 0.7 to 7.0 at.%. This is a strong indication that the 3.2-eV absorption line is due to a Pb dimer state.

Luminescence due to isolated Pb atoms in SrS has been observed previously.³ In that work emission and excitation spectra of polycrystalline films of SrS:Pb were presented. A narrow impurity emission line at 3.35 eV was observed. The peak energy for exciting that luminescence was 3.54 eV. This is most likely the same Pb transition as was observed here. No mention is made of Pb dimers in Ref. 3. A much broader emission line was found centered at 4.05 eV. This emission may be due to the indirect energy gap predicted in Ref. 2. As noted earlier, we were unable to detect any corresponding feature in our absorption spectra.

Luminescence features in CaS:Pb and CaSe:Pb have been ascribed to aggregates of Pb ions.⁴ In those materials a Pb monomer transition was also observed. At large Pb content a series of lines appeared at lower energy. The lines grew rapidly in intensity as the Pb content was further increased. These lines appeared in CaSe:Pb only when the Pb concentration approached 0.5 at.%. They were visible in CaS:Pb at concentrations as low as 0.01 at.%. The dimer transition energies calculated in Ref. 4 agree well with those experimental results.

When the $\text{Pb}_{1-x}\text{Sr}_x\text{S}$ samples are cooled from 300 to 80 K the band gap increases by roughly 50 meV. The discrete absorption lines appeared to move with the absorption edge. It is notable that the lines do not move with the band gap edge as E_g varies with composition. Upon cooling, the full width at half maximum (FWHM) of the 3.5-eV line decreases from 160 meV at 300 K to 100 meV at 80 K. This is consistent with the semiclassical $\coth^{1/2}(\hbar\omega/kT)$ dependence due to interaction with optical phonons.⁵

The improved definition of the peaks at low temperature reveals a third, very small absorption peak at 3.1 eV. This third peak is discernible only in samples with $x \leq 0.95$. We tentatively assign this feature to one or more of several possible Pb trimer configurations.

THEORY

It is convenient to describe the Pb impurity states in a simple tight-binding model. We adapt the work of Pantelides⁶ for this purpose. Since the Pb interacts with the surrounding S atoms, it is necessary to obtain the parameters for this interaction as well as the sulfur-sulfur interactions. This we do first, and then compare our results with other approaches.

The valence bands of SrS are composed mostly of the S 3p orbitals. Nearest anion neighbors interact with a p-bonding matrix element V_p and a π -bonding V_π . These parameters can be determined by fitting, for example, the $\Gamma_{15^-}X_5'$ and $\Gamma_{15^-}X_4'$ energy differences [Fig. 4(a) is a schematic drawing of the band structure of SrS]. These were calculated in Ref. 2 and were found to be

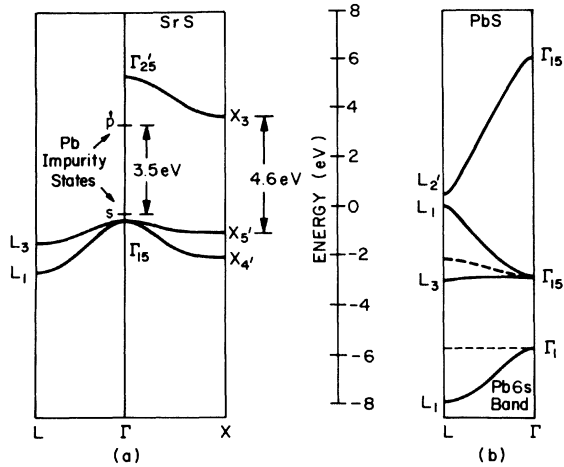


FIG. 4. (a) Schematic band diagram of SrS. The general structure is drawn from the results of Ref. 2. However, the X_3 - X_5 band gap has been adjusted to the measured value of 4.6 eV. The symmetry labels denote irreducible representations about the Sr atoms. Impurity states in the gap due to Pb are shown. The s state is the antibonding state referred to in the text. The Pb 6s level (not shown) is below the valence band. (b) Schematic band diagram of PbS drawn from Ref. 7. The dashed curves show the positions of the bands leading to the L_1 state when $V_{sp}=0$.

$$E(\Gamma_{15}) - E(X_{5'}) = 4(V_p - 3V_\pi) = 0.45,$$

$$E(\Gamma_{15}) - E(X_{4'}) = 8(V_p - V_\pi) = 1.42,$$

in units of eV. Solving these equations gives $V_p = 0.210$ eV and $V_\pi = 0.325$ eV. It appears that the L_1 and L_3 levels are pushed down somewhat due to interactions with the conduction bands and cannot be used to estimate V_p and V_π . Otherwise, it is assumed that the Sr levels are high enough in energy that they may be neglected.

The Pb cation, however, has a 6s level just below the valence band. It interacts with the nearest-neighbor S anions with a matrix element V_{sp} .⁶ We can estimate V_{sp} from the band structure of PbS.⁷ A schematic of the band structure of Pb is shown in Fig. 4(b). The Pb 6s band is pushed down at the L point due to its interaction via V_{sp} with the top of the valence band. The valence band is pushed up an equal amount [see dashed curves in Fig. 4(b)]. In nonrelativistic notation the energy splitting between the two L_4 -symmetric states is given by

$$E_v(L_1) - E_s(L_1) = \{ [E_v^{(0)}(L_1) - E_s^{(0)}(L_1)]^2 + 48V_{sp}^2 \}^{1/2}.$$

We must now determine the positions of the L_1 states in the absence of interaction before solving for V_{sp} .

At Γ , the S p states are Γ_{15} and the Pb s states are Γ_1 which do not interact. We attribute all the dispersion between Γ_1 and L_1 to V_{sp} . Therefore, we identify $E_s^{(0)}(L_1)$ with the Γ_1 energy, -5.7 eV. Since $E_s(L_1) = -7.9$ eV, this implies a shift of 2.2 eV and puts $E_v^{(0)}(L_1)$ at -2.2 eV [where $E_v(L_1) \equiv 0$]. We therefore find from the equations above that $V_{sp} = 1.02$ eV. The S 3p energy E_p can be determined from the relationship⁶

$$E_v^{(0)}(L_1) = E_p - 4(V_p - V_\pi).$$

(Note that in Ref. 6 L_1 is labeled L_2' , because the origin was chosen as the anion rather than the usual choice of the cation.) This gives $E_p = -1.23$ eV. The Pb 6s energy is $E_s = -5.7$ eV.

To find the energy level of a single Pb impurity in the SrS lattice it is helpful to consider first a cluster of six S atoms surrounding a Pb. The symmetric states can be found easily. The wave function is a linear combination of the Pb 6s state and the S 3p states, e.g., the $\pm p_x$ orbital centered at $(\pm a/2, 0, 0)$ where a is the lattice constant. The eigenvalue equation is

$$(E_s - E)A_s + 6V_{sp}A_p = 0,$$

$$V_{sp}A_s + (E_p - E)A_p = 0.$$

The energies of the bonding and antibonding states are

$$E = \frac{1}{2}(E_s + E_p) \pm \frac{1}{2}[(E_s - E_p)^2 + 24V_{sp}^2]^{1/2}.$$

For our estimates of the parameter involved, we find $E = -6.82$ and -0.11 eV. The latter represents the (occupied) impurity state of interest since it is in the gap [$E(\Gamma_{15}) = E_p + 4(V_p - 2V_\pi)$ is the top of the SrS valence band at -0.65 eV with the present definition of energy origin]. It has s -like (or A_1) symmetry and is localized primarily on the S atoms (A_s^2 is only 0.2). The bonding state at -6.82 eV corresponds to the hyperdeep trap state in the nomenclature of Hjalmarson *et al.*⁸

It has long been recognized⁹ that for ns^2 ions (e.g., Tl^+ , which has the same configuration as Pb^{2+}) in alkali halides the ns level is raised considerably compared to the free ion. This has been attributed to the Madelung potential and to interactions of the ion with the surrounding halogen ions. For our model of Pb in SrS, we have concluded that there is a substantial hybridization of the 6s levels and the anion p levels.

For a crystal of SrS containing a Pb impurity, we find the energy of the occupied impurity state to be -0.42 eV, compared to -0.11 eV as calculated for the cluster. Again we neglect any interaction with the Sr ions. This calculation uses the Haydock recursion method¹⁰ and will be described elsewhere.¹¹ The impurity state is calculated to be 0.23 eV above the top of the valence band and 0.68 eV above X_5 . The direct gap is thought to be the X_5 to X_3 transition.

The upper (unoccupied) state of the discrete transition is obviously a p -like state derived from the Pb 6p orbitals. In PbS the 6p orbitals are in the conduction band. If our estimate of the energy for the s -like state is correct, the p -like state must fall at $-0.42 + 3.5 = 3.08$ eV. This is consistent with the location of the PbS conduction bands. The conduction-band edge of SrS is at 3.50 eV on this scale. Using the tight-binding parameters obtained from a fit to the PbS band structure, we can calculate the energy for the impurity p level.¹¹ In a crystal the recursion method gives 4.07 eV which is above the SrS conduction-band edge. However, this is probably close to the correct one-electron level because the actual transition energy is affected by the exchange splitting. We believe the ob-

served monomer peak to be due to the A band^{3,9} or 1S to 3P transition (allowed by the spin-orbit interaction). The C band or 1S to 1P transition occurs above the fundamental gap (4.6 eV) of SrS. Our value of $4.07 + 0.42 = 4.49$ eV for the s to p transition should represent the centroid of the A and C bands. The C band is observed in CaS because the fundamental gap is larger.⁴ The energies of the Pb impurity states are included in the SrS band schematic in Fig. 4(a).

In the alkali halides, dimers of thallos ions have been observed.¹² Peaks in the absorption spectrum occur below both the A and C bands. The intensity of these peaks varies with the square of the impurity concentration. The same lowering of the dimer energies obtains for Pb in CaS.⁴ The question of geometrical arrangement, i.e., either a [110] dimer or a [100] dimer, has not been settled. In our one-electron calculations we find the [100] dimer has a transition energy of 3.36 eV, which is close to the observed 3.2 eV. The calculated lowering of the dimer energy is due mostly to the interaction through the S atoms separating the Pb atoms. The energies of the [110] dimer, on the other hand, do not differ much from the monomer because there is no S separating the Pb ions. The direct Pb-Pb interaction does not appear to be appreciable. Hence, our tentative conclusion is that the 3.2-eV peak in Fig. 1 is due to [100] dimers. The absorption due to [110] dimers falls under the monomer peak at 3.5 eV.

Note added in proof. Throughout this and earlier work

(Ref. 1), the optical-absorption edge has been interpreted as arising from a direct energy gap that decreased very rapidly as Pb was substituted for Sr in SrS. More recent studies suggest that this interpretation is invalid for material with composition close to pure SrS ($x \approx 1$). Optical-absorption spectra of very thin ($\sim 0.05 \mu\text{m}$) specimens of (Pb,Sr)S have yielded data at higher photon energy than was previously possible. With pure SrS, an exciton absorption peak has been resolved at 4.9 eV. Substitution of up to 20 at. % of the metal with Pb did not significantly shift the exciton energy. However, the change in composition did result in an absorption tail extending to lower photon energy, in agreement with previous experimental data. These results are consistent with an interpretation in which the direct energy gap between the valence and the conduction bands is insensitive to composition for $x > 0.8$. The observed rapid decrease in the energy of the optical-absorption edge is due to the formation of a Pb impurity band within the energy gap. This interpretation is consistent with the theoretical results of Ref. 11.

ACKNOWLEDGMENTS

The authors thank Dr. E. P. O'Reilly for a copy of the Cambridge Recursion Library, Ms. E. Ho and Professor J. D. Dow for a band-structure program, and Mr. R. Ager for his expert technical assistance.

¹H. Holloway and J. Jasion, Phys. Rev. B **26**, 5617 (1982).

²A. Hasegawa and A. Yanase, J. Phys. C **13**, 1995 (1980).

³A. F. Ellervee, Phys. Status Solidi B **82**, 91 (1977).

⁴S. Asano, N. Yamashita, and Y. Nakao, Phys. Status Solidi B **89**, 663 (1978).

⁵K. Schmitt, V. S. Sivasankar, and P. W. M. Jacobs, J. Phys. C **16**, 615 (1983); Y. Toyozawa and M. Inoue, J. Phys. Soc. Jpn. **21**, 1663 (1966).

⁶S. T. Pantelides, Phys. Rev. B **11**, 5082 (1975).

⁷S. E. Kohn, P. Y. Yu, Y. Petroff, Y. R. Shen, Y. Tsang, and M.

L. Cohen, Phys. Rev. B **8**, 1477 (1973).

⁸H. P. Hjalmarson, P. Vogl, D. J. Wolford, and J. D. Dow, Phys. Rev. Lett. **44**, 810 (1980).

⁹F. Seitz, J. Chem. Phys. **6**, 150 (1938).

¹⁰R. Haydock, in *Solid State Physics*, edited by H. Ehrenreich, F. Seitz, and D. Turnbull, (Academic, New York, 1980), Vol. 35, p. 215.

¹¹L. C. Davis (unpublished).

¹²T. Tsubai, J. Phys. Soc. Jpn. **29**, 1303 (1970).